Journal of Hydrology 556 (2018) 1232–1243

Contents lists available at ScienceDirect

Journal of Hydrology

journal homepage: www.elsevier.com/locate/jhydrol

Research papers

Spatial connections in regional climate model rainfall outputs at different temporal scales: Application of network theory

Ihsan Naufan [a], Bellie Sivakumar [a,b,*], Fitsum M. Woldemeskel [a], Srivatsan V. Raghavan [c], Minh Tue Vu [c,d], Shie-Yui Liong [c,e]

[a] School of Civil and Environmental Engineering, The University of New South Wales, Sydney, NSW 2052, Australia
[b] Department of Land, Air and Water Resources, University of California, Davis, CA 95616, USA
[c] Tropical Marine Science Institute, National University of Singapore, Singapore 119227, Singapore
[d] Glenn Department of Civil Engineering, Clemson University, Clemson, SC 29634, USA
[e] Willis Research Network, Willis Re Inc., London EC3M 7DQ, United Kingdom

ARTICLE INFO

Article history:
Available online 19 May 2017

Keywords:
Rainfall
Scaling
Regional climate models
Complex networks
Clustering coefficient
Degree distribution

ABSTRACT

Understanding the spatial and temporal variability of rainfall has always been a great challenge, and the impacts of climate change further complicate this issue. The present study employs the concepts of complex networks to study the spatial connections in rainfall, with emphasis on climate change and rainfall scaling. Rainfall outputs (during 1961–1990) from a regional climate model (i.e. Weather Research and Forecasting (WRF) model that downscaled the European Centre for Medium-range Weather Forecasts, ECMWF ERA-40 reanalyses) over Southeast Asia are studied, and data corresponding to eight different temporal scales (6-hr, 12-hr, daily, 2-day, 4-day, weekly, biweekly, and monthly) are analyzed. Two network-based methods are applied to examine the connections in rainfall: clustering coefficient (a measure of the network's local density) and degree distribution (a measure of the network's spread). The influence of rainfall correlation threshold (T) on spatial connections is also investigated by considering seven different threshold levels (ranging from 0.5 to 0.8). The results indicate that: (1) rainfall networks corresponding to much coarser temporal scales exhibit properties similar to that of small-world networks, regardless of the threshold; (2) rainfall networks corresponding to much finer temporal scales may be classified as either small-world networks or scale-free networks, depending upon the threshold; and (3) rainfall spatial connections exhibit a transition phase at intermediate temporal scales, especially at high thresholds. These results suggest that the most appropriate model for studying spatial connections may often be different at different temporal scales, and that a combination of small-world and scale-free network models might be more appropriate for rainfall upscaling/downscaling across all scales, in the strict sense of scale-invariance. The results also suggest that spatial connections in the studied rainfall networks in Southeast Asia are weak, especially when more stringent conditions are imposed (i.e. when T is very high), except at the monthly scale.

1. Introduction

The rainfall process exhibits considerable amount of spatial and temporal variability, due to prevailing climatic conditions, rainfall generating mechanisms, and topographic properties, among others. As a result, rainfall modeling is, in general, a challenging task. With the past, present, and future impacts of global climate change on rainfall, including in the form of significant changes in frequency, magnitude, and intensity, rainfall modeling will likely become far more challenging in the future; see, for example, Dai et al. (1997), Zhang et al. (2007), Trenberth (2011), and Donat et al. (2016) for some details.

There exist numerous approaches for studying the spatial and temporal variability of rainfall, including those based on correlation, trend, linearity vs. nonlinearity, stationarity vs. nonstationarity, determinism vs. stochasticity, scaling or fractal, dimensionality, entropy, and many other properties (e.g. Eagleson, 1967; Waymire and Gupta, 1981; Berndtsson, 1988; Krstanovic and Singh, 1992; Onof and Wheater, 1993; Salas et al., 1995; Carsteanu and Foufoula-Georgiou, 1996; Deidda, 2000; Sivakumar et al., 2001; Molnar and Burlando, 2005; Langousis and Veneziano, 2007; Bárdossy and Pegram, 2009; Li et al., 2013;

* Corresponding author at: School of Civil and Environmental Engineering, The University of New South Wales, Sydney, NSW 2052, Australia.
E-mail address: s.bellie@unsw.edu.au (B. Sivakumar).

http://dx.doi.org/10.1016/j.jhydrol.2017.05.029
0022-1694/

Niu, 2013; Liew et al., 2014; Poornima and Jothiprakash, 2015). Although such approaches and their applications have significantly enhanced our understanding of rainfall variability, there is still a long way to go in our quest to achieve reliable outcomes in rainfall modeling. What is also clear is that new approaches, including those that can supplement and complement the existing ones, are clearly needed. To this end, new developments in some other scientific fields can, as they often do, provide useful avenues. One such field is the field of complex systems science, especially considering that hydroclimatic systems are inherently complex systems with many components that are highly interconnected and governed by nonlinear interactions, feedbacks, self-organization, scale, thresholds, emergence, and sensitive dependence on initial conditions, among other properties.

Among the new developments in the field of complex systems science, developments in network theory, and *complex networks* in particular (e.g. Watts and Strogatz, 1998; Barabási and Albert, 1999; Girvan and Newman, 2002; Milo et al., 2002), have been found to be very useful for studying the spatial and temporal evolution of a wide range of complex systems and associated phenomena; see, for example, Watts (1999), Barabási (2002), and Estrada (2012) for comprehensive accounts. As the concepts of *complex networks* have obvious relevance in hydrology and water resources, their applications in this field have been gaining attention in recent years (e.g. Rinaldo et al., 2006; Zaliapin et al., 2010; Suweis et al., 2011; Malik et al., 2012; Scarsoglio et al., 2013; Sivakumar and Woldemeskel, 2014; Braga et al., 2016; Serinaldi and Kilsby, 2016; Fang et al., 2017), including for studying connections in rainfall, streamflow, river networks, and virtual water trade networks; see Sivakumar (2015) for a general account.

In the specific context of rainfall, a few recent studies have applied the concepts of complex networks. For instance, Malik et al. (2012) applied several complex networks-based methods (degree centrality, degree distribution, clustering coefficient, and closeness centrality) to examine the spatial and temporal characteristics of extreme (summer) monsoonal rainfall over South Asia. They analyzed daily gridded rainfall data over the period 1951–2007 from the Asian Rainfall Highly Resolved Observational Data Integration Towards the Evaluation of Water Resources (APHRODITE) project (Yatagai et al., 2009). Boers et al. (2013) applied networks-based concepts to investigate the spatial characteristics of extreme rainfall synchronicity of the South American Monsoon System (SAMS), by analyzing gridded daily rainfall data (1999–2012) with a spatial resolution of $0.25^\circ \times 0.25^\circ$, obtained from the Tropical Rainfall Measuring Mission (TRMM) 3B42 V7 satellite product; see also Boers et al. (2014, 2015) for subsequent complex networks-based studies on South American rainfall. Scarsoglio et al. (2013) applied several complex networks-based methods (degree centrality, clustering coefficient, degree distribution, and shortest path length) to examine the spatial dynamics of annual precipitation around the globe. They analyzed a 70-year long (January 1941–December 2010) gridded precipitation data from the Global Precipitation Climatology Center (GPCC) Database. Sivakumar and Woldemeskel (2015) employed the concepts of clustering coefficient and degree distribution to examine the spatial connections in rainfall in Australia, by analyzing monthly rainfall observed over a period of 68 years (1940–2007) at 230 raingage stations across Australia. They also studied the influence of rainfall correlation threshold on the outcomes of clustering coefficient and degree distribution methods. Jha et al. (2015) attempted to offer hydrologic explanation for the outcomes of the complex networks-based methods for rainfall. They applied the clustering coefficient method to two different raingage networks in Australia (57 stations from Western Australia and 45 stations from the Sydney region) and interpreted the results in terms of topographic properties of raingage stations (latitude, longitude, and elevation) and characteristics of rainfall data (mean, standard deviation, and coefficient of variation).

With the encouraging outcomes reported by these studies on the suitability and usefulness of complex networks for rainfall analysis, the present study attempts to advance research in this direction further. Specifically, the study focuses on two aspects: (1) investigation of spatial connections in rainfall data from a regional climate model, in the context of climate change; and (2) examination of the effects of temporal scale on rainfall connections, in the context of scaling or scale-invariance. Rainfall outputs over the period 1961–1990 (a period that is generally used as the 'current climate' in the context of climate change) from the Weather Research and Forecasting (WRF) model that downscaled the European Centre for Medium-range Weather Forecasts (ECMWF) ERA-40 reanalyses data over Southeast Asia are studied; see Uppala et al. (2005) for details of the ERA-40 reanalyses datasets. For examination of the influence of temporal scale on connections, rainfall data corresponding to eight different scales are considered: 6-hr, 12-hr, 24-hr (daily), 48-hr (2-day), 96-hr (4-day), 168-hr (weekly), 336-hr (biweekly), and 720-hr (monthly – 30 days). While the primary criterion in the selection of these different scales is to represent successively-doubled resolutions to facilitate interpretations linking scale and connections, some coarser scales are also chosen to coincide with weekly, biweekly, and monthly scales, in view of practical considerations in terms of water planning and management. Two complex networks-based methods are employed to study the connections in these rainfall data: clustering coefficient (a measure of the network's local density) and degree distribution (a measure of the network's spread). The influence of rainfall correlation thresholds on the connections is also studied.

The rest of this paper is organized as follows. Section 2 explains the concept of a network and the procedure for calculation of clustering coefficient and degree distribution. Section 3 presents details of the study area and rainfall data considered. Analysis, results, and discussion are reported in Section 4, followed by conclusions in Section 5.

2. Networks, clustering coefficient, and degree distribution

2.1. Network

A *network* (or a *graph*) is a set of points connected together by a set of lines, as shown in Fig. 1. The points are called *nodes* or *vertices*, and the lines are called *links* or *edges*. Mathematically, a network can be represented as $G = \{P,E\}$, where P is a set of N nodes ($P_1,P_2,\ldots,P_N$) and E is a set of n links. Networks can have many different forms, such as networks: (1) with identical nodes and links; (2) with more than one different type of node and/or link; (3) with different weights for different nodes and links; (4) with links that can be directed (either cyclic or acyclic); (5) with multilinks, self-links, or hyperlinks; and (6) that are bipartite. Some additional details on these can be found in Sivakumar (2015).

There exist a large number of measures to study the properties of complex networks; see Newman (2010) and Estrada (2012) for details. The measures include centrality, clustering, adjacency, distance, community structure, bipartivity, fragments (or subgraphs), communicability, and global invariants, among others. While these different measures identify/quantify different properties of networks, they also often provide cross-verification of results. For some measures, there are also different definitions, sub-measures, and corresponding methods. For example, clustering coefficient is used as an indicator of clustering properties, and degree distribution is used as an indicator of adjacency properties. These two are described below, as they are employed in the present study for studying the connections in rainfall data.

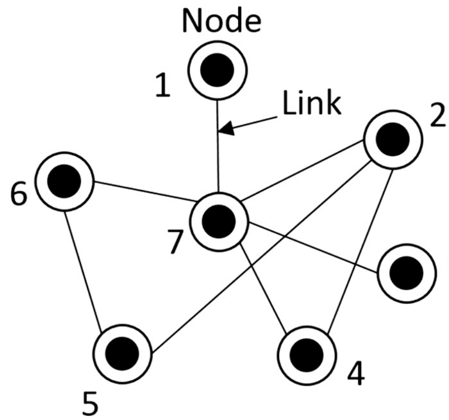

Fig. 1. Concept of a network.

2.2. Clustering coefficient

One of the most fundamental properties of networks is their tendency to cluster. The concept of clustering has its origin in sociology, under the name *fraction of transitive triples* (e.g. Wasserman and Faust, 1994). However, in the context of complex networks, Watts and Strogatz (1998) were the first to use the clustering concept. The tendency of a network to cluster is quantified by the clustering coefficient. There exist several definitions of clustering coefficient; see Watts and Strogatz (1998), Barrat and Weigt (2000), and Newman (2001) for details. However, the clustering coefficient method proposed by Watts and Strogatz (1998), which measures the local density, is very widely used. A brief description of its calculation is presented here; see Sivakumar and Woldemeskel (2014) for an example.

Let us consider a node i in a network and that it has k_i links (identified based on some criterion, such as correlation) which connect it to k_i other nodes, as shown in Fig. 2 (left). This is what is normally done in most of the traditional 'similarity-based' approaches (such as those based on distance or correlation or other measures) to identify the existence of connections between nodes (e.g. rainfall stations). The clustering coefficient method involves another step. In this, first the 'initial connections' are identified by determining 'similar' nodes based on some property (as is done in traditional approaches – Fig. 2(a)), and then the 'actual connections' are identified by looking into the connections among those 'similar' nodes. That is, if the neighbors of the original node i were part of a cluster, there would be $k_i(k_i-1)/2$ links between them, as shown in Fig. 2 (right). With this, the clustering coefficient of node i is the ratio between the number E_i of links that actually exist between these k_i nodes (solid lines) and the total number $k_i(k_i-1)/2$ (all lines), given by:

$$C_i = \frac{2E_i}{k_i(k_i-1)} \tag{1}$$

This way, the strength of connections in the network is identified in a much better way, which allows studying the system as a whole, rather than through its parts (e.g. just one-to-one connection between nodes). The procedure is then repeated for each node of the network. The clustering coefficient of the whole network, C, is then given by the average of the clustering coefficients of all the individual nodes.

The clustering coefficient of the individual nodes and of the entire network can be used to obtain important information about the type of network, grouping (or classification) of nodes, and identification of dominant nodes (e.g. super nodes), among others. For instance, a very high clustering coefficient (close to 1.0) indicates a regular network, while a very low clustering coefficient (close to zero), with $C = p$ (where p is the probability that every pair of nodes is connected equally), indicates a classical random network (see Erdös and Rényi, 1959, 1960). The clustering coefficient of, for example, a small-world network (e.g. Watts and Strogatz, 1998) and a scale-free network (e.g. Barabási and Albert, 1999) is generally smaller than that of the regular network but also larger than that of a comparable classical random network (i.e. having the same number of nodes and links). The clustering coefficient value can also be used to make a further distinction between small-world networks and scale-free networks. In general, small-world networks have relatively much higher clustering coefficients than those of scale-free networks. However, there are exceptions to such an interpretation, since, for example, some scale-free networks can have high clustering coefficients.

It is important to note that both the small-world networks and the scale-free networks are also random networks. However, they have different forms and properties when compared to the classifical random networks; see Albert and Barabási (2002) for details. The small-world networks start with a fixed number of nodes (like classifical random networks), are stable with significantly high clustering coefficient (unlike classical random networks), and are efficient (like classifical random networks). The scale-free networks, unlike classical random networks, start with a few nodes and grow by the continuous addition of new nodes, exhibit preferential attachment, and display power-law degree distribution (i.e. a few nodes with high degree and a large proportion of nodes with relatively low degree); see Section 2.3 for further details on degree distribution.

2.3. Degree distribution

In a network, several structural properties are related to adjacency relationships between nodes. There are different ways to measure the adjacency relations, including node adjacency, degree distribution, degree-degree correlation, and link adjacency. Among these, the degree distribution is a particularly useful measure (e.g. Barabási and Albert, 1999), especially for the identification of the type of network, and is widely used in network studies.

In a network, different nodes may have different number of links. The number of links (k) of a node is called as *node degree*. The spread in the node degrees is characterized by a distribution function, $p(k)$, which expresses the fraction of nodes in a network with degree k. This distribution is called *degree distribution*, and is often a reliable indicator of the type of network. For instance, in a purely random graph, since the links are placed randomly, the majority of nodes have approximately the same degree, and close to the average degree $\bar{k}$ of the network. Therefore, the degree distribution of a completely random graph is a Poisson distribution, given by:

$$p(k) = \frac{e^{-\bar{k}}\bar{k}^k}{k!} \tag{2}$$

However, scale-free networks are characterized by a few nodes of high degree and a large proportion of nodes with relatively low degree (Barabási and Albert, 1999). Although such networks can display a wide range of 'fat-tail' degree distributions, the easiest way of conceptualizing such characteristics is to consider power-law degree distribution, given by:

$$p(k) \sim k^{-\gamma} \tag{3}$$

where γ is the degree exponent. In other words, a model in which the probability of finding a node with degree k decreases as a power-law of its degree. Similarly, depending upon the properties

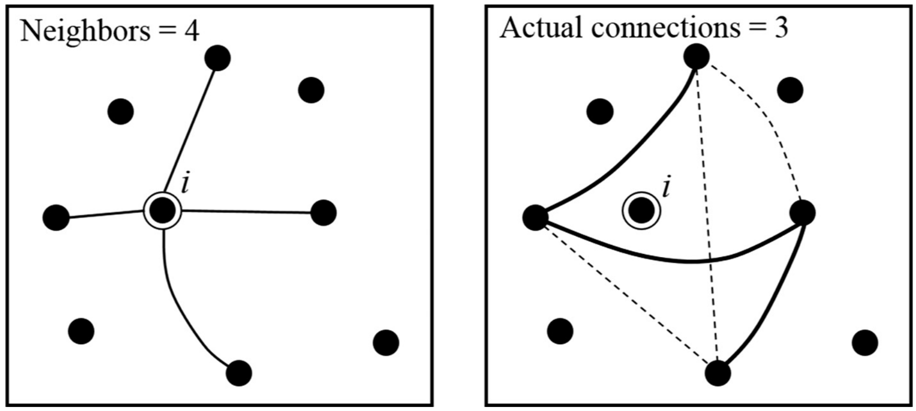

Fig. 2. Connections in a network and calculation of clustering coefficient.

of networks, degree distribution can be, for example, Gaussian, exponential, or other, or even a combination of any of the above.

Among these distributions, the power-law or scale-free distribution has attracted considerable attention in the literature on complex networks, as such has been found in a large number of natural and social networks (e.g. Barabási and Albert, 1999; Kim et al., 2004; Keller, 2005; Clauset et al., 2010). The fractal or scale-free nature of numerous natural and social systems and their ability also to self-organize themselves, already well-documented in the literature (e.g. Mandelbrot, 1983; Bak, 1996; Rodriguez-Iturbe and Rinaldo, 1997; Barnsley, 2012), certainly give credence and motivation to further advance research on scale-free networks. The scale-free nature of networks has particular relevance in the present study, both for the scale-free nature of rainfall (e.g. Lovejoy and Mandelbrot, 1985; Gupta and Waymire, 1993; Carsteanu and Foufoula-Georgiou, 1996; Puente and Obregon, 1996; Deidda, 2000; Sivakumar et al., 2001; Veneziano et al., 2006; Langousis and Veneziano, 2007; Özger et al., 2010; Langousis et al., 2013) and for the analysis of rainfall network corresponding to different temporal scales studied herein to examine connections at such scales.

3. Study area and data

In the present study, connections in rainfall dynamics in Southeast Asia are investigated using the concepts of complex networks. The study region considered herein spans between 79°58′58″E to 132°1′2″E longitude and 19°26′54″S to 26°48′16″N latitude (see Fig. 3). This region covers almost all of Southeast Asia, some parts of South Asia and China (and territories), a very small part of northern Western Australia, as well as parts of the Indian ocean that lie within this region.

The climate over much of this region is mainly tropical, being generally hot and humid throughout the year with significant amounts of rainfall. Some parts of the region, however, have a sub-tropical climate, with cold winter with some snow. Seasonal shifts in winds or monsoon cause wet and dry seasons over a majority of this region. The tropical rain belt causes additional rainfall during the monsoon season. The rain forest in this region is the oldest and the second largest in the world, next only in size to that of the Amazon. An exception to this type of climate and vegetation is the mountain areas in the northern parts, where high altitudes lead to milder temperatures and drier landscape.

The rainfall data considered in this study are obtained from a 30 km $\times$ 30 km climate simulations of a regional climate model (Weather Research and Forecasting, WRF) downscaling of the global ERA-40 reanalyses datasets (Uppala et al., 2005); see also http://www.ecmwf.int/research/era/. The ERA-40 reanalyses, developed by the European Centre for Medium-range Weather Forecasts (ECMWF), UK, provide information about a suite of climate variables, including rainfall, humidity, temperature, and pressure, at every 6-hr, at a horizontal resolution of 2.5° $\times$ 2.5°. For rainfall, the ERA-40 reanalyses data are made available for the period 1957–2002.

In the present study, the WRF model downscaled rainfall data for the period 1961–1990 over Southeast Asia are investigated for spatial connections using clustering coefficient and degree distribution methods. The data are first extracted from the above-mentioned regional climate model simulations. The extraction of the time series is done through bilinear interpolation; see Liew et al. (2014) for additional details. For each grid (30 km $\times$ 30 km), there are approximately 43,800 values of 6-hr data (i.e. 30 years $\times$ 365 days $\times$ 4 values per day). Some other studies that have used this data for rainfall analyses over Southeast Asia are Liew et al. (2014), Vu et al. (2014), and Raghavan et al. (2015).

To assess the influence of temporal scale on rainfall connections, data corresponding to different scales are analyzed. To this end, in addition to the original 6-hr data, seven other coarser scales are also considered: 12-hr, 24-hr (daily), 48-hr (2-day), 96-hr (4-day), 168-hr (weekly), 336-hr (biweekly), and 720-hr (monthly – 30 days). All these scales are chosen in such a way that they: (1) are useful to link the temporal scale of rainfall data and spatial connections (particularly in terms of scale-invariance); and (2) have practical relevance in terms of short-term emergency measures (e.g. floods) as well as medium- to long-term management strategies (e.g. water supply).

4. Analysis, results, and discussion

The clustering coefficient and the degree distribution methods are applied to rainfall data over Southeast Asia, for each of the eight different temporal scales. For each temporal scale, each grid serves as a node in the network, with each node consisting of a time series of rainfall at that particular scale. The existence/non-existence of links in the network is identified using the Pearson correlation coefficient of rainfall between the different nodes. For instance, if the Pearson correlation coefficient between two nodes exceeds an assumed threshold (T), then there is a link between the two nodes; otherwise, the link does not exist. It is important to note that the outcomes of the clustering coefficient and degree distribution methods can be significantly influenced by the correlation threshold (T) used for identification of neighbors (i.e. links); see Sivakumar and Woldemeskel (2014, 2015) and Jha et al. (2015) for additional details. In view of this, different threshold values are considered to assess their influence and interpret the results. Keeping in mind the range of temporal scales considered (i.e. 6-hr to

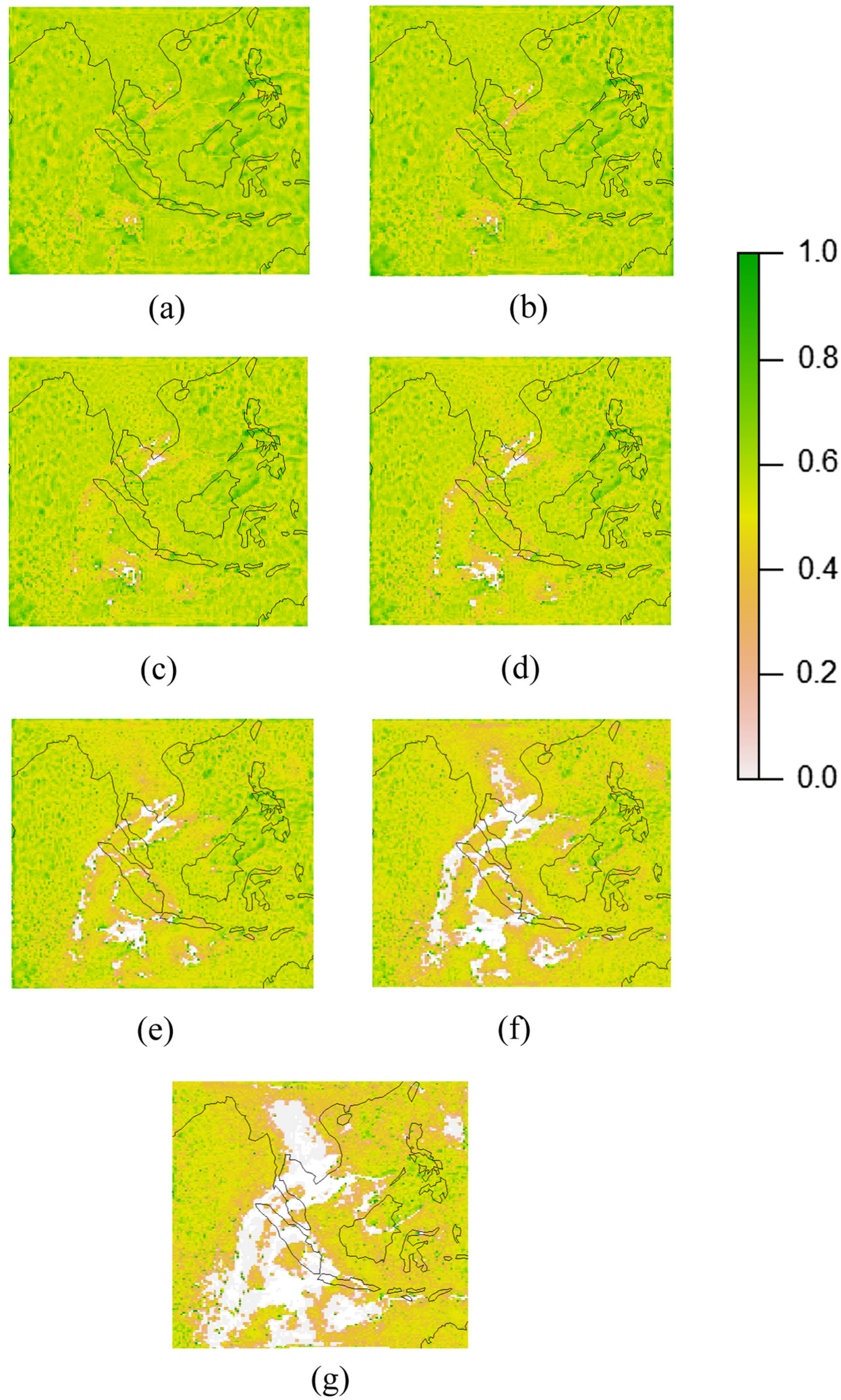

Fig. 3. Clustering coefficient values for 2-day rainfall over 25,872 grids in Southeast Asia, for seven different threshold levels (T): (a) $T = 0.50$; (b) $T = 0.55$; (c) $T = 0.60$; (d) $T = 0.65$; (e) $T = 0.70$; (f) $T = 0.75$; and (g) $T = 0.80$.

monthly) and the possible extent of variability in spatial correlations on one hand and the computational time required to implement the methods on the other, seven different threshold values are considered: 0.5, 0.55, 0.6, 0.65, 0.7, 0.75, and 0.8. Therefore, with eight temporal scales and seven correlation thresholds, there is a total of 56 rainfall networks to analyze.

4.1. Clustering coefficient

Fig. 3(a)–(g) presents, for example, the clustering coefficient (CC) values obtained for the rainfall network when the 2-day temporal scale is considered, for the seven different thresholds, respectively. As normally expected, for any given node (i.e. grid) and, consequently, for the whole network, the clustering coefficient generally decreases with an increase in the threshold. When the threshold is low (say, $T \leq 0.55$; Fig. 3(a) and (b)), most of the grids have high clustering coefficient values (say, CC $\geq$ 0.60); see the green[1] color for much of the study region. When the threshold is high (say, $T \geq 0.75$; Fig. 3(f) and (g)), most of the grids have low clustering coefficient values (say, CC $\leq$ 0.40); see the red and also the white colors (including very low and even zero CC values) over a significant part of the study region, especially in the middle. At intermediate thresholds, most of the grids have intermediate clustering coefficient values; see a combination of green and red colors over much of the region. The clustering coefficient value for the entire network at the 2-day scale is 0.598, 0.590, 0.579, 0.563, 0.537, 0.494, and 0.418 for T = 0.50, 0.55, 0.60, 0.65, 0.70, 0.75, and 0.80, respectively.

Fig. 4(a)–(h) presents, for example, the clustering coefficient results for the rainfall network corresponding to the eight temporal scales, respectively, when the threshold level is 0.6. For any given node and, consequently, for the whole network, the clustering coefficient generally increases with an increase in the temporal scale. At very fine temporal scales (say, 6-hr and 12-hr scales; Fig. 4(a) and (b)), most of the grids have low clustering coefficient values (say, CC $\leq$ 0.40), and this is particularly the case in the middle of the study region. At very coarse temporal scales (say, biweekly and monthly scales; Fig. 4(g) and (h)), most of the grids have high clustering coefficient values (say, CC $\geq$ 0.60). At intermediate temporal scales (daily to weekly scales; Fig. 4(c)–(f)), most of the grids have intermediate clustering coefficient values. Considering the entire networks corresponding to the eight temporal scales, the clustering coefficient value consistently increases from 0.376 at the 6-hr scale to 0.629 at the monthly scale.

Table 1 and Fig. 5 summarize the clustering coefficient results obtained for the 56 rainfall networks (i.e. eight temporal scales and seven thresholds). The results generally indicate a negative relationship between clustering coefficient and threshold level and a positive relationship between clustering coefficient and temporal scale. That is, for any given temporal scale, the clustering coefficient decreases with an increase in the threshold (Fig. 5(a)); for any given threshold, the clustering coefficient increases with an increase in the temporal scale (Fig. 5(b)). These general observations are along expected lines. However, the clustering coefficient results also reveal some specific observations as to the nature and extent of connections in rainfall with respect to temporal scale and threshold.

As the results in Table 1 indicate, the clustering coefficient values range anywhere from as low as 0.163 (for 6-hr scale at T = 0.75) to as high as 0.635 (for monthly scale at T = 0.5), considering the eight temporal scales and seven correlation thresholds. Considering a clustering coefficient value $\geq$ 0.50 as a reasonably medium to high value, the CC values obtained for the different networks, and especially their differences between the different networks, have some important implications, such as:

1. None of the 56 rainfall networks is a purely (i.e. classical) random network (since the clustering coefficient should be close to 0.0 for a purely random graph) or a regular network (since the clustering coefficient should be close to 1.0 for a fully-connected network). The networks are of some other type, such as small-world or scale-free or other (see Section 2).
2. When the threshold level is low (say, $T \leq 0.55$), all the networks (except one: 6-hr scale at T = 0.55) have medium to high clustering coefficients (CC $\geq$ 0.45), regardless of the temporal scale, and may be classified as small-world networks. When the threshold level is high (say, $T \geq 0.70$), there are significant differences in clustering coefficients between networks corresponding to different temporal scales. Networks that correspond to coarser temporal scales (say, scale $\geq$ 4-day) have medium to high clustering coefficients and may be classified as small-world networks, while networks that correspond to finer temporal scales (say, scale < 4-day) have low clustering coefficients and may be classified as scale-free networks or some other.
3. All networks that correspond to coarser temporal scales (say, scale $\geq$ 4-day), with medium to high clustering coefficients, seem to belong to the small-world network type, regardless of the threshold level. However, networks that correspond to finer scales (say, scale $\leq$ 12-hr) exhibit very different clustering coefficients, depending upon the threshold. Such networks may be classified as small-world networks when the threshold is low and scale-free networks (or other) when the threshold is high. Networks that correspond to intermediate temporal scales (say, daily and 2-day scales) and intermediate thresholds (say, T = 0.6 and 0.65) seem to belong to small-world networks as well.

These observations seem to suggest that the spatial connections in rainfall are different at different temporal scales. In terms of the strength of connections in the rainfall network (reflected by the clustering coefficient), there are clear differences between very coarse scales (say, scale $\geq$ 4-day, and especially $\geq$ weekly) and very fine scales (say, scale $\leq$ 12-hr), including in the nature of the network; that is, small-world network in the former and scale-free network in the latter. The differences are particularly evident at very high threshold levels (say, $T \geq 0.70$). The clustering coefficient results also suggest a transition phase in the strength of spatial connections corresponding to intermediate temporal scales, i.e. at daily and 2-day scales. This transition is, again, particularly evident at very high threshold levels ($T \geq 0.70$) and, to a certain extent, at medium threshold levels (T = 0.6 and 0.65).

All these results have important implications for scaling-based studies in rainfall, including in the identification of appropriate scales and models for upscaling/downscaling of rainfall. For instance, rainfall upscaling/downscaling may be more effective within very coarse scales (say, scale $\geq$ 4-day, and especially $\geq$ weekly) and within very fine scales (say, scale $\leq$ 12-hr), but not between or across them, since a noticeable transition seems to occur between these scales. This is particularly the case when high accuracy in upscaling/downscaling is expected or needed (including for flood forecasting), as clearly reflected by the noticeable differences in the strength of spatial connections (i.e. clustering coefficients) between very coarse scales and very fine scales at very high threshold levels. As the results also suggest, the appropriate model for studying spatial connections at different scales may also be different. For instance, models based on scale-free concepts seem to be more appropriate for very fine temporal scales, while models based on small-world concepts seem to be more appropriate for very coarse temporal scales. Therefore, perhaps, a combination of small-world and scale-free models might be more appropriate for the transition phase of temporal scales and for rainfall upscaling/downscaling across all scales (whether in time or space or space-time), in the strict sense of scale-invariance.

To illustrate further the strength of spatial connections in rainfall in the study region, Fig. 6 presents the percentage of grids that have very high clustering coefficient values, i.e. CC > 0.85. As normally expected, the percentage of grids decreases with an increase in the threshold value (Fig. 6(a)) and increases with an increase in the temporal scale (Fig. 6(b)). However, the actual values reveal

[1] For interpretation of color in Figs. 3 and 4, the reader is referred to the web version of this article.

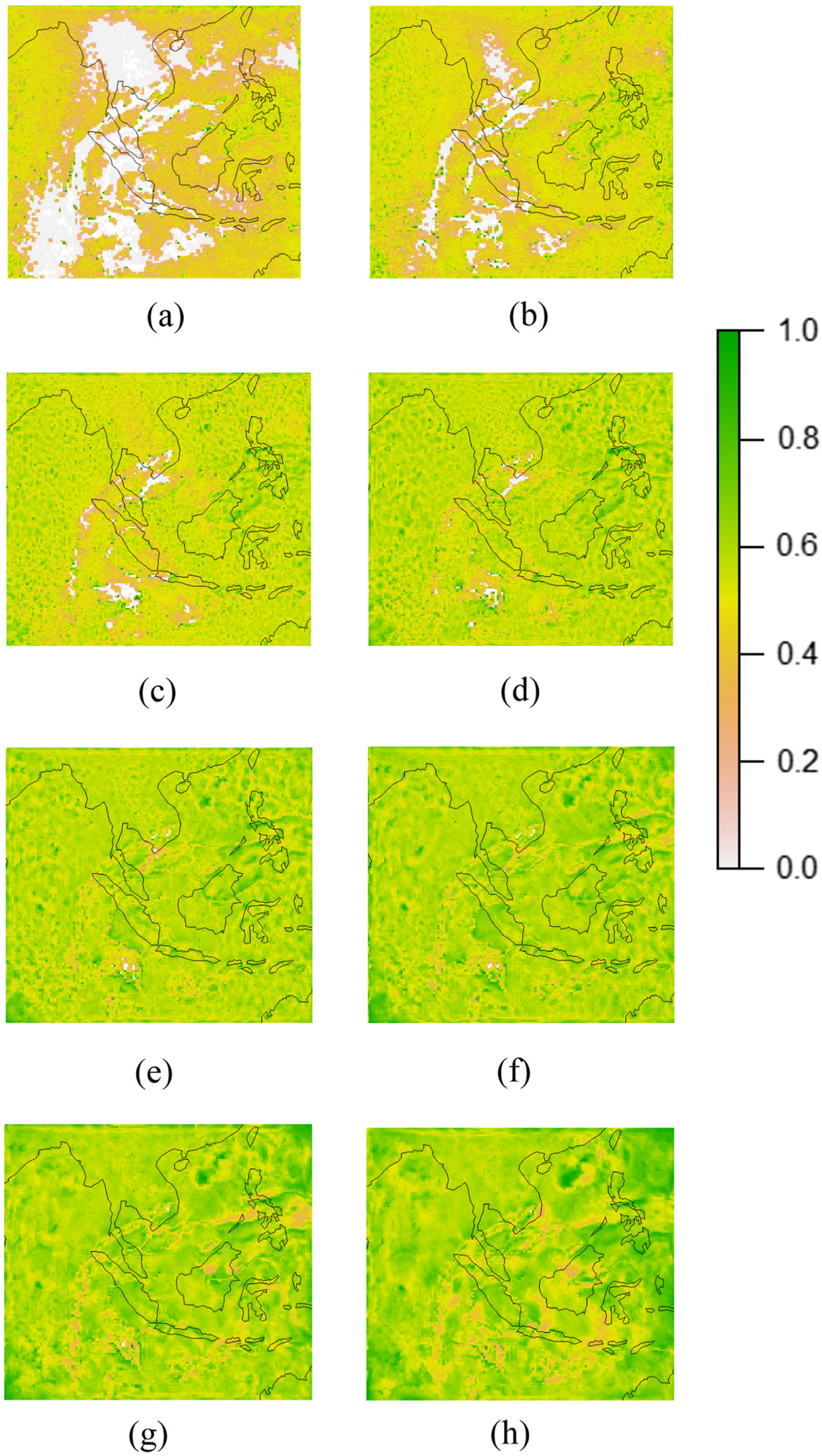

Fig. 4. Clustering coefficient values for rainfall over 25,872 grids in Southeast Asia at eight different temporal scales: (a) 6-hr; (b) 12-hr; (c) daily; (d) 2-day; (e) 4-day; (f) Weekly; (g) Biweekly; and (g) Monthly. The values correspond to a threshold level (T) of 0.60.

some interesting observations. Regardless of the temporal scale and threshold value, only less than 3.5% of the grids have CC > 0.85 (see Fig. 6(a)). Indeed, the number of grids with CC > 0.85 exceeds 2% only for the coarsest scale (monthly). For all the other seven temporal scales (i.e. daily to biweekly), the number of grids with CC > 0.85 is less than 2%, and is even less than 1% in

Table 1
Clustering coefficients for rainfall data at different temporal scales for different correlation thresholds (T).

Time Scale	Threshold (T)						
	0.5	0.55	0.6	0.65	0.7	0.75	0.8
6 h	0.498	0.450	0.376	0.273	0.193	0.163	0.176
12 h	0.548	0.524	0.485	0.429	0.336	0.231	0.173
1 day	0.579	0.565	0.546	0.515	0.466	0.388	0.270
2 days	0.599	0.590	0.579	0.563	0.538	0.494	0.419
4 days	0.609	0.605	0.598	0.588	0.572	0.547	0.501
Weekly	0.615	0.613	0.608	0.601	0.590	0.572	0.540
Biweekly	0.621	0.619	0.617	0.613	0.606	0.593	0.571
Monthly	0.635	0.632	0.629	0.624	0.618	0.610	0.596

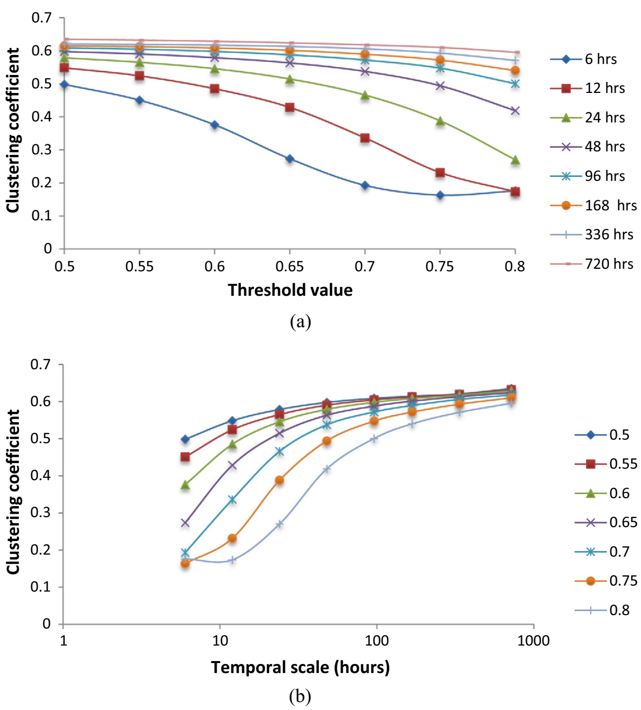

Fig. 5. Average (or global) clustering coefficient values for 56 different rainfall networks in Southeast Asia: (a) Clustering coefficient vs. threshold, for different temporal scales; and (b) Clustering coefficient vs. temporal scale, for different thresholds.

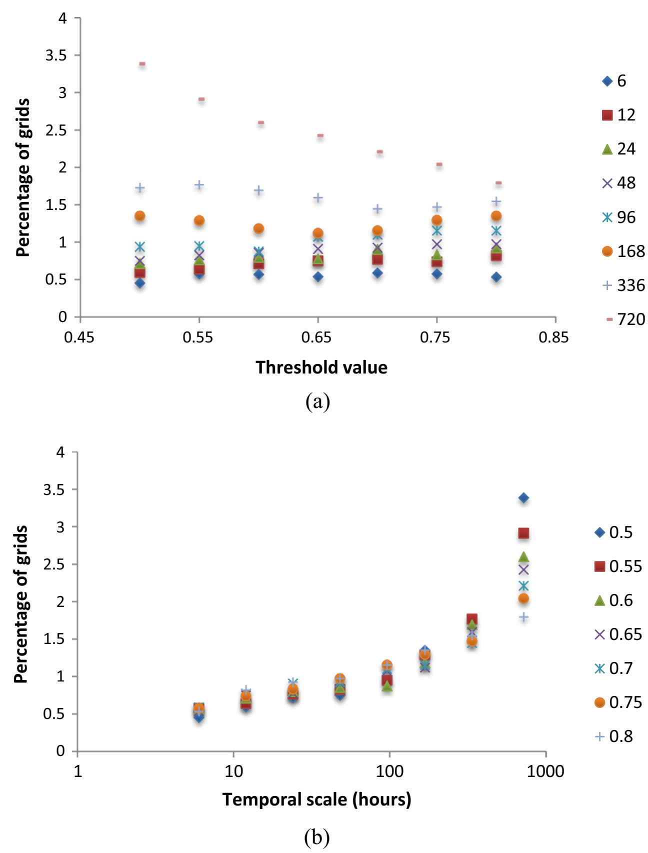

Fig. 6. Percentage of rainfall grids in Southeast Asia having clustering coefficients ≥0.86, for 56 rainfall networks in Southeast Asia: (a) Percentage of grids vs. threshold, for different temporal scales; and (b) Percentage of grids vs. temporal scale, for different thresholds.

most cases. In terms of the threshold, the number of grids with CC > 0.85 is less than 2% even for thresholds down to as low as 0.5, except for the monthly scale (Fig. 6(b)). These observations suggest that the spatial connections in all the studied rainfall networks are weak, perhaps with the exception of the monthly scale.

4.2. Degree distribution

Fig. 7(a)–(n) presents the degree distribution results for rainfall networks at the eight different temporal scales (in each plot, left to right in increasing order of magnitude), for the seven different thresholds (top to bottom plots in increasing order of magnitude). The values are the complementary cumulative degree distribution values, defined as the fraction of nodes with degree at least k and denoted as $p(K \geq k)$. The plots show the results in the normal scale (left-side plots) and log-log scale (right-side plots). The degree distribution results reveal the following:

1. For any given threshold, the degree distribution exhibits a general trend. Rainfall networks corresponding to very coarse temporal scales (say, scale ≥ weekly) exhibit a distribution that is more similar to exponential (and perhaps small-world networks). Rainfall networks corresponding to very fine temporal scales (say, scale ≤ 12-hr) exhibit a distribution that is more similar to power-law (and perhaps scale-free networks). Rainfall networks corresponding to intermediate temporal scales exhibit a distribution that is somewhat of a combination of exponential (perhaps small-world) and power-law (perhaps scale-free) distributions.
2. The exponential distribution for rainfall networks at very coarse temporal scales is more evident at low thresholds (say, $T \leq 0.55$; Fig. 7(a) to (d)). When the threshold is high (say, $T \geq 0.75$; Fig. 7(k)–(n)), the exponential distribution (perhaps small-world network) is not that evident and the distribution seems to approach a power-law behavior (perhaps scale-free network).

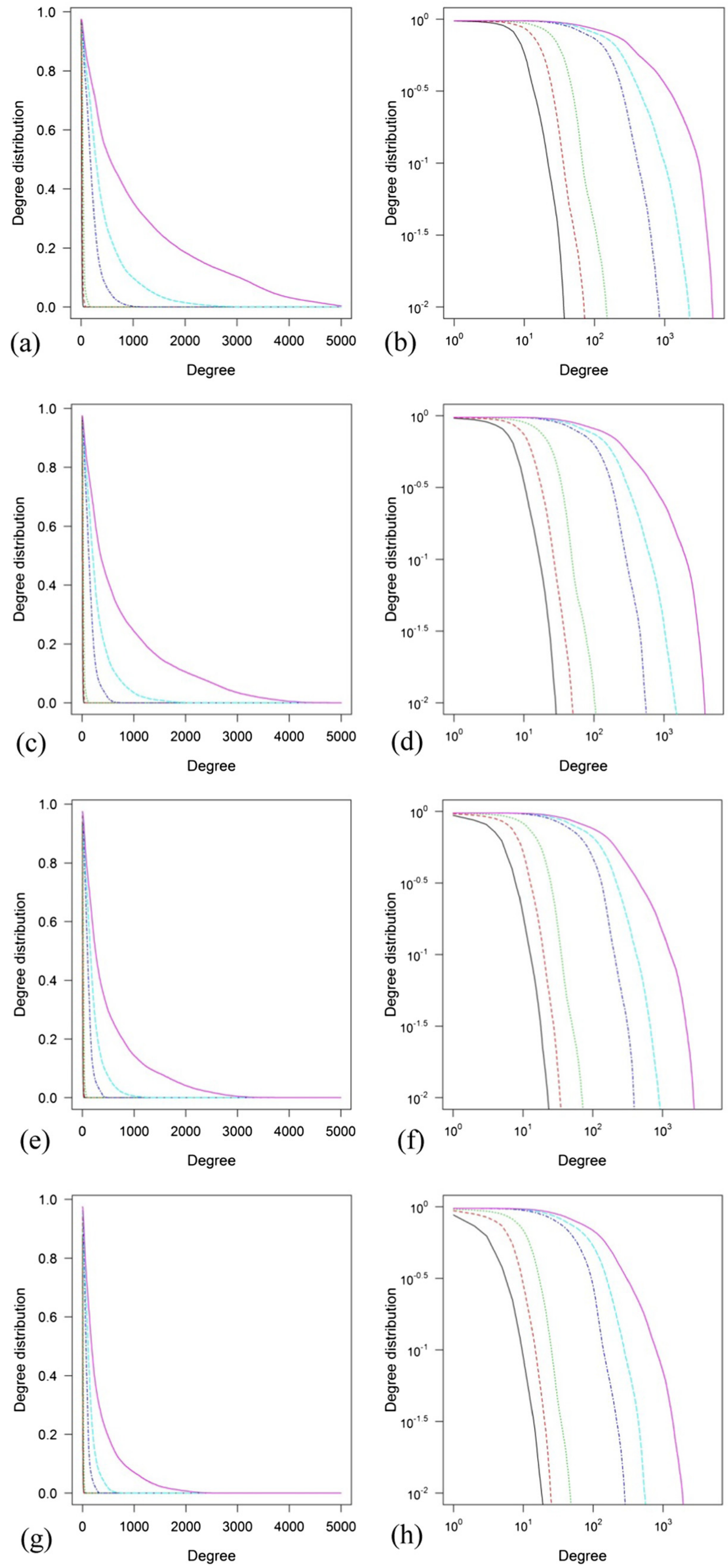

Fig. 7. Degree distribution for rainfall networks in Southeast Asia. The results are presented in normal scale (left) and log-log scale (right). The results are for seven different threshold levels (T = 0.50, 0.55, 0.60, 0.65, 0.70, 0.75, 0.80), from top to bottom, in increasing order of magnitude. Each plot presents results for eight different temporal scales (6-hr, 12-hr, daily, 2-day, 4-day, weekly, biweekly, and monthly), from left to right, in increasing order of magnitude.

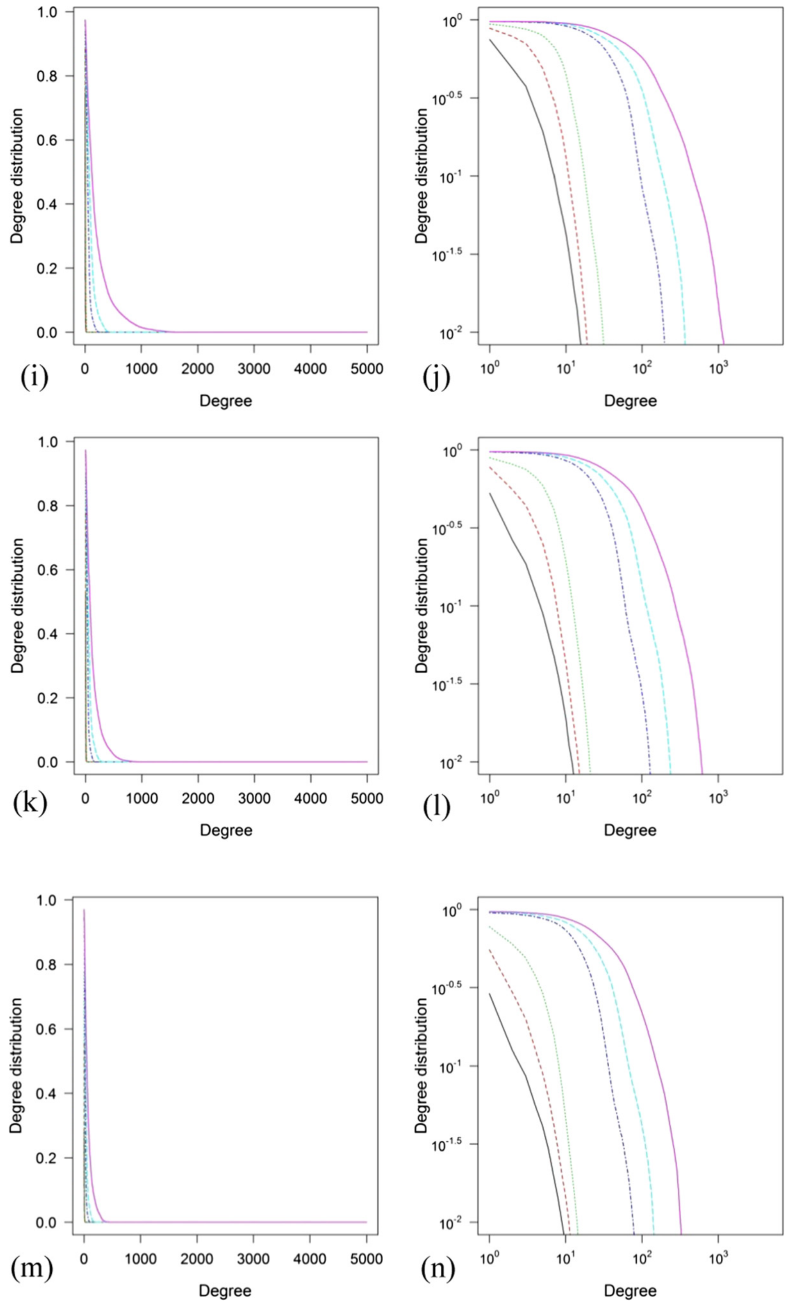

Fig. 7 (*continued*)

3. For very fine temporal scales (say, scale ≤ 12-hr), while the distribution of the rainfall networks seems to be similar and power-law behavior (perhaps scale-free network) for any threshold, the power-law distribution is more evident at high thresholds (say, $T \geq 0.75$; Fig. 7(k)–(n)) when compared to that at low thresholds (say, $T \leq 0.55$; Fig. 7(a)–(d)). At low thresholds, the distribution seems to deviate from power-law behavior (perhaps scale-free network) towards exponential behavior (perhaps small-world network).

These observations seem to suggest that a power-law distribution (perhaps scale-free network) is more fitting for very fine temporal scales and an exponential distribution (perhaps small-world network) is more fitting for very coarse temporal scales, while their combination is more fitting for intermediate temporal scales. These observations are consistent with those made using the clustering coefficients, in that the rainfall spatial connections at very coarse temporal scales exhibit one type of behavior (small-world) and those at very fine temporal scales exhibit another type of behavior (scale-free), while connections at the intermediate temporal scales exhibit a combination of exponential (and perhaps small-world) and power-law (and perhaps scale-free) behaviors and, thus, a transient phase. Further, none of the 56 rainfall networks (56 combinations of temporal scale and threshold level) exhibit a degree distribution that is similar to Poisson (or Gaussian), suggesting that the networks are not classical random networks.

The results presented in Fig. 7 also indicate that, even considering the lowest threshold level, i.e. $T = 0.50$, even the most connected grid is connected with only less than 19% of the network size. When far more stringent conditions in connections are imposed (say, $T = 0.80$), even the most connected grid is connected with only less than 2% of the network size. These results again suggest that the spatial connections in the rainfall networks are generally weak, and thus support the results from the clustering coefficient method. In other words, any of the grids in the rainfall network (including the grid that has the most connection) has only very little influence on the network as a whole, despite the fact that power-law distribution is observed for rainfall networks at finer temporal scales. These observations have implications for rainfall studies, including in the context of upscaling/downscaling and interpolation/extrapolation of rainfall.

5. Conclusions

The present study has applied the concepts of complex networks to study the connections in rainfall outputs from a regional climate model. Application of the clustering coefficient and degree distribution methods to rainfall in Southeast Asia during the period 1961–1990 ('current climate') and at different temporal scales (ranging from 6-hr to monthly) has provided some interesting results about the connections in rainfall. The results indicate that the properties of spatial connections in rainfall are different at different temporal scales and also influenced by the correlation threshold (T). The connections at much coarser temporal scales (scale $\geq$ weekly) exhibit properties similar to that of small-world networks, regardless of the threshold. At much finer temporal scales (scale $\leq$ 12-hr), the threshold plays an important role, with spatial connections exhibiting properties of either small-world networks (for low thresholds) or scale-free networks (at high thresholds). The connections at intermediate scales exhibit a transition phase, especially at high thresholds. Overall, the spatial connections in rainfall in Southeast Asia are weak, especially when more stringent conditions are imposed (i.e. when T is very high), except at the monthly scale.

The present results have important implications for studies on rainfall variability, rainfall scaling, and related aspects. First, the different network properties at different temporal scales imply that the appropriate model for studying spatial connections may be different at different temporal scales. Second, the transition phase in spatial connections at intermediate temporal scales implies "breaking points" or "critical points" in rainfall behavior. Third, combination of small-world and scale-free network models seems more appropriate for rainfall modeling across all scales, in the strict sense of scale-invariance. The implications of the present results can be particularly realized in the context of climate change, since climate change is anticipated to significantly change the frequency, magnitude, and intensity of rainfall and, hence, the properties of spatial connections across different temporal scales.

The present study leads to several future directions of research: (1) Application of complex networks concepts to rainfall data obtained from ground measurements to examine the consistency of results with those obtained in the present study with RCM rainfall outputs; (2) Study of future rainfall projections from climate models to check whether the present results (on network properties) would still hold for future conditions; and (3) Development of a rainfall model that can represent both small-world network properties and scale-free network properties of spatial connections at different temporal scales, i.e. space-time network model. Research in these directions are currently underway, and the details will be reported elsewhere.

Finally, one of the eventual purposes in studying spatial connections in rainfall (at one or more temporal scales) is to estimate rainfall data at ungagged locations, using interpolation (or extrapolation) methods. Although the present study provides some interesting results about spatial connections in rainfall at different temporal scales and helps identify suitable complex networks-based models, it does not actually develop any new model. Developing a complex networks-based model (whether in space or in time or in space-time) for rainfall networks and its proper use for rainfall interpolation will be important future steps in research in this direction. Comparison of the performance of such a complex networks-based model with that of existing methods for rainfall interpolation (e.g. nearest neighbors and their variants, splines, kriging) would be a necessary and appropriate endeavor, to assess the superiority of such a model, if any. This, however, is beyond the scope of the present study. We indeed intend to address this in our future studies.

Acknowledgments

This project is supported by the Australian Research Council (ARC). Bellie Sivakumar acknowledges the financial support from ARC through the Future Fellowship grant (FT110100328). Srivatsan Raghavan, Minh Tue Vu, and Shie-Yui Liong thank the Center for Environmental Modeling and Sensing (CENSAM), SMART, Singapore and the Centre for Hazards Research, Department of Civil and Environmental Engineering, National University of Singapore for providing the resources for supercomputing. We thank the two anonymous reviewers and the Associate Editor for their constructive comments on earlier versions of this manuscript, which helped improve the quality and presentation of our work.

References

Albert, R., Barabási, A.-L., 2002. Statistical mechanics of complex networks. Rev. Modern Phys. 74, 47–97.
Bak, P., 1996. How Nature Works: The Science of Self-Organized Criticality. Springer-Verlag, New York, p. 212.
Barabási, A.-L., 2002. Linked: The New Science of Networks. Perseus, Cambridge, MA, USA.
Barabási, A.-L., Albert, R., 1999. Emergence of scaling in random networks. Science 286, 509–512.
Bárdossy, A., Pegram, G.G.S., 2009. Copula based multisite model for daily precipitation simulation. Hydrol. Earth Syst. Sci. 13, 1361–1373.
Barnsley, F.M., 2012. Fractals Everywhere. Dover Publications, Mineola, NY.
Barrat, A., Weigt, M., 2000. On the properties of small-world networks. Eur. Phys. J. B 13, 547–560.
Berndtsson, R., 1988. Temporal variability in spatial correlation of daily rainfall. Water Resour. Res. 24 (9), 1511–1517.
Boers, N., Bookhagen, B., Marwan, N., Kurths, J., Marengo, J., 2013. Complex networks identify spatial patterns of extreme rainfall events of the South American Monsoon System. Geophys. Res. Lett. 40 (1–7), 4386–4392. http://dx.doi.org/10.1002/grl.50681.
Boers, N., Rheinwalt, A., Bookhagen, B., Barbosa, H.M.J., Marwan, N., Marengo, J., Kurths, J., 2014. The South American rainfall dipole: a complex network analysis of extreme events. Geophys. Res. Lett. 41, 7397–7405. http://dx.doi.org/10.1002/2014GL061829.
Boers, N., Bookhagen, B., Marengo, J., Marwan, N., von Storch, J.-S., Kurths, J., 2015. Extreme rainfall of the South American Monsoon System: a dataset comparison using complex networks. J. Climate 28, 1031–1056.
Braga, A.C., Alves, L.G.A., Costa, L.S., Ribeiro, A.A., de Jesus, M.M.A., Tateishi, A.A., Ribeiro, H.V., 2016. Characterization of river flow fluctuations via horizontal visibility graphs. Phys. A 444, 1003–1011.
Carsteanu, A., Foufoula-Georgiou, E., 1996. Assessing dependence of weights in a multiplicative cascade model of temporal rainfall. J. Geophys. Res. 101, 26363–26370.
Clauset, A., Rohilla Shalizi, C., Newman, M.E.J., 2010. Power-law distribution in empirical data. SIAM Rev. 51, 661–703.
Dai, A., Fung, I.Y., Del Genio, A.D., 1997. Surface observed global land precipitation variation during 1900–88. J. Clim. 10, 2943–2962.
Deidda, R., 2000. Rainfall downscaling in a space-time multifractal framework. Water Resour. Res. 36 (7), 1779–1784.
Donat, M.G., Lowry, A.L., Alexander, L.V., O'Gorman, P.A., Maher, N., 2016. More extreme precipitation in the world's dry and wet regions. Nat. Climate Change 6, 508–513.
Eagleson, P.S., 1967. Optimum density of rainfall networks. Water Resour. Res. 3, 1021–1033.
Erdös, P., Rényi, A., 1959. On random graphs. I. Publ. Math. (Debrecen) 6, 290–297.
Erdös, P., Rényi, A., 1960. On the evolution of random graphs. Publ. Math. Inst. Hung. Acad. Sci. 5, 17–61.
Estrada, E., 2012. The Structure of Complex Networks: Theory and Applications. Oxford University Press, Oxford, UK.
Fang, F., Sivakumar, B., Woldemeskel, F.M., 2017. Complex networks, community structure, and catchment classification in a large-scale river basin. J. Hydrol. 545, 478–493.

Girvan, M., Newman, M.E.J., 2002. Community structure in social and biological networks. Proc. Natl. Acad. Sci. U.S.A. 99, 7821–7826.
Gupta, V.K., Waymire, E.C., 1993. A statistical-analysis of mesoscale rainfall as a random cascade. J. Appl. Meteorol. 32, 251–267.
Jha, S.K., Zhao, H., Woldemeskel, F.M., Sivakumar, B., 2015. Network theory and spatial rainfall connections: an interpretation. J. Hydrol. 527, 13–19.
Keller, E.F., 2005. Revisiting 'scale-free' networks. BioEssay 27, 1060–1068.
Kim, D.-H., Noh, J.D., Jeong, H., 2004. Scale-free trees: the skeletons of complex networks. Phys. Rev. E 70, 046126.
Krstanovic, P.F., Singh, V.P., 1992. Evaluation of rainfall networks using entropy: II. Appl. Wat. Resour. Manage. 6, 295–314.
Langousis, A., Veneziano, D., 2007. Intensity-duration-frequency curves from scaling representations of rainfall. Water Resour. Res. 43. http://dx.doi.org/10.1029/2006WR005245.
Langousis, A., Carsteanu, A.A., Deidda, R., 2013. A simple approximation to multifractal rainfall maxima using a generalized extreme value distribution model. Stoch. Environ. Res. Risk Assess. 27 (6), 1525–1531.
Li, Z., Yang, D., Hong, Y., 2013. Multi-scale evaluation of high-resolution multi-sensor blended global precipitation products over the Yangtze River. J. Hydrol. 500, 157–169.
Liew, S.C., Raghavan, S.V., Liong, S.-Y., 2014. How to construct future IDF curves, under changing climate, for sites with scarce rainfall records. Hydrol. Process. 28 (8), 3276–3287.
Lovejoy, S., Mandelbrot, B., 1985. Fractal properties of rain and a fractal model. Tellus 37A, 209–232.
Malik, N., Bookhagen, B., Marwan, N., Kurths, J., 2012. Analysis of spatial and temporal extreme monsoonal rainfall over South Asia using complex networks. Clim. Dyn. 39, 971–987.
Mandelbrot, B.B., 1983. The Fractal Geometry of Nature. W.H. Freeman and Company, New York.
Milo, R., Shen-Orr, S., Itzkovitz, S., Kashtan, N., Chklovskii, D., Ulon, U., 2002. Network motifs: simple building blocks of complex networks. Science 298, 824–827.
Molnar, P., Burlando, P., 2005. Preservation of rainfall properties in stochastic disaggregation by a simple random cascade model. Atmos. Res. 77 (1–4), 137–151.
Newman, M.E.J., 2001. The structure of scientific collaboration networks. Proc. Nat. Acad. Sci. USA 98, 404–409.
Newman, M.E.J., 2010. Networks: An Introduction. Oxford University Press, Oxford, UK.
Niu, J., 2013. Precipitation in the Pearl River basin, South China: scaling, regional patterns, and influence of large-scale climate anomalies. Stoch. Environ. Res. Risk Assess. 27 (5), 1253–1268.
Onof, C., Wheater, H.S., 1993. Modeling of British rainfall using a random parameter Bartlett-Lewis rectangular pulse model. J. Hydrol. 146, 67–95.
Özger, M., Mishra, A.K., Singh, V.P., 2010. Scaling characteristics of precipitation data in conjunction with wavelet analysis. J. Hydrol. 395, 279–288.
Poornima, U., Jothiprakash, V., 2015. Extraction of trend of rainfall using singular spectrum analysis. J. Hydrol. Eng. 20 (12), 05015007.
Puente, C.E., Obregon, N., 1996. A deterministic geometric representation of temporal rainfall. Results for a storm in Boston. Water Resour. Res. 32 (9), 2825–2839.
Raghavan, S.V., Vu, M.T., Liong, S.Y., 2015. Regional climate simulations over Vietnam using the WRF model. Theor. Appl. Clim. http://dx.doi.org/10.1007/s00704-015-1557-0.
Rinaldo, A., Banavar, J.R., Maritan, A., 2006. Trees, networks, and hydrology. Water Resour. Res. 42. http://dx.doi.org/10.1029/2005WR004108. W06D07.
Rodriguez-Iturbe, I., Rinaldo, A., 1997. Fractal River Networks: Chance and Self-Organization. Cambridge University Press, New York.
Salas, J.D., Delleur, J.W., Yevjevich, V., Lane, W.L., 1995. Applied Modeling of Hydrologic Time Series. Water Resources Publications, Littleton, Colorado, USA.
Scarsoglio, S., Laio, F., Ridolfi, L., 2013. Climate dynamics: a network-based approach for the analysis of global precipitation. PLoS ONE 8 (8), e71129. http://dx.doi.org/10.1371/journal.pone.0071129.
Serinaldi, F., Kilsby, C.G., 2016. Irreversibility and complex network behavior of stream flow fluctuations. Phys. A 450, 585–600.
Sivakumar, B., 2015. Networks: a generic theory for hydrology? Stoch. Environ. Res. Risk Assess. 29, 761–771.
Sivakumar, B., Woldemeskel, F.M., 2014. Complex networks for streamflow dynamics. Hydrol. Earth Syst. Sci. 11, 7255–7289.
Sivakumar, B., Woldemeskel, F.M., 2015. A network-based analysis of spatial rainfall connections. Environ. Modell. Softw. 69, 55–62.
Sivakumar, B., Sorooshian, S., Gupta, V.K., Gao, X., 2001. A chaotic approach to rainfall disaggregation. Water Resour. Res. 37 (1), 61–72.
Suweis, S., Konar, M., Dalin, C., Hanasaki, N., Rinaldo, A., Rodriguez-Iturbe, I., 2011. Structure and controls of the global virtual water trade network. Geophys. Res. Lett. 38, L10403. http://dx.doi.org/10.1029/2011GL046837.
Trenberth, K.E., 2011. Changes in precipitation with climate change. Clim. Res. 47, 123–138.
Uppala, S.M., Kållberg, P.W., Simmons, A.J., Andrae, U., da Costa, B.V., Fiorino, M., Gibson, J.K., Haseler, J., Hernandez, A., Kelly, G.A., Li, X., Onogi, K., Saarinen, S., Sokka, N., Allan, R.P., Andersson, E., Arpe, K., Balmaseda, M.A., Beljaars, A.C.M., van de Berg, L., Bidlot, J., Bormann, N., Caires, S., Chevallier, F., Dethof, A., Dragosavac, M., Fisher, M., Fuentes, M., Hagemann, S., Hólm, E., Hoskins, B.J., Isaksen, L., Janssen, P.A.E.M., Jenne, R., McNally, A.P., Mahfouf, J.-F., Morcrette, J.-J., Rayner, N.A., Saunders, R.W., Simon, P., Sterl, A., Trenberth, K.E., Untch, A., Vasiljevic, D., Viterbo, P., Woollen, J., 2005. The ERA-40 reanalysis. Quart. J. R. Meteorol. Soc. 131, 2961–3012.
Veneziano, D., Langousis, A., Furcolo, P., 2006. Multifractality and rainfall extremes: a review. Water Resour. Res. 42. http://dx.doi.org/10.1029/2005WR004716.
Vu, M.T., Raghavan, S.V., Pham, D.M., Liong, S.Y., 2014. Investigating drought over the Central Highland, Vietnam, using regional climate models. J. Hydrol. 526, 265–273.
Wasserman, S., Faust, K., 1994. Social Network Analysis. Cambridge University Press, Cambridge.
Watts, D.J., 1999. Small Worlds: The Dynamics of Networks Between Order and Randomness. Princeton University Press, Princeton.
Watts, D.J., Strogatz, S.H., 1998. Collective dynamics of 'small-world' networks. Nature 393, 440–442.
Waymire, E., Gupta, V.K., 1981. The mathematical structure of rainfall representations, 2, A review of the theory of point processes. Water Resour. Res. 17 (5), 1273–1286.
Yatagai, A., Arakawa, O., Kamiguchi, K., Kawamoto, H., 2009. A 44 year daily gridded precipitation dataset for Asia based on dense network of rain gauges. SOLA 5, 137–140.
Zaliapin, I., Foufoula-Georgiou, F., Ghil, M., 2010. Transport on river networks: a dynamic tree approach. J. Geophys. Res. 115. http://dx.doi.org/10.1029/2009JF001281. F00A15.
Zhang, X., Zwiers, F.W., Hegerl, G.C., Hugo Lambert, F., Gillet, N.P., Solomon, S., Stott, P.A., Nozawa, T., 2007. Detection of human influence on twentieth-century precipitation trends. Nature 448, 461–466.